

Asymmetric Blockade and Multiqubit Gates via Dipole-Dipole Interactions

Jeremy T. Young^{1,2,3,*}, Przemyslaw Bienias^{1,3,4}, Ron Belyansky^{1,3,4}, Adam M. Kaufman¹, and Alexey V. Gorshkov^{1,3,4}¹*JILA, University of Colorado and National Institute of Standards and Technology, and Department of Physics, University of Colorado, Boulder, Colorado 80309, USA*²*Center for Theory of Quantum Matter, University of Colorado, Boulder, Colorado 80309, USA*³*Joint Quantum Institute, NIST/University of Maryland, College Park, Maryland 20742 USA*⁴*Joint Center for Quantum Information and Computer Science, NIST/University of Maryland, College Park, Maryland 20742 USA*

(Received 21 July 2020; revised 11 May 2021; accepted 13 July 2021; published 17 September 2021)

Because of their strong and tunable interactions, Rydberg atoms can be used to realize fast two-qubit entangling gates. We propose a generalization of a generic two-qubit Rydberg-blockade gate to multiqubit Rydberg-blockade gates that involve both many control qubits and many target qubits simultaneously. This is achieved by using strong microwave fields to dress nearby Rydberg states, leading to asymmetric blockade in which control-target interactions are much stronger than control-control and target-target interactions. The implementation of these multiqubit gates can drastically simplify both quantum algorithms and state preparation. To illustrate this, we show that a 25-atom Greenberger-Horne-Zeilinger state can be created using only three gates with an error of 5.8%.

DOI: 10.1103/PhysRevLett.127.120501

Strong, tunable interactions between Rydberg states have positioned neutral atoms as a versatile platform for quantum information science and quantum simulations. Many of these proposed applications rely on Rydberg blockade, a process in which a single Rydberg excitation prevents nearby atoms from being excited to the Rydberg state. In recent years, there have been extensive efforts to characterize and improve the performance of entangling two-qubit gates based on Rydberg blockade, first proposed in Ref. [1] and further investigated in Refs. [2–4]. This novel approach was later followed by a variety of theoretical extensions [5–18] and experimental implementations [19–25]. Recently, two-qubit entangling gates have been realized experimentally with high fidelities [26–30].

The long-range character of Rydberg van der Waals (vdW) and dipole-dipole interactions opens the possibility of engineering entangling gates involving many qubits. Although two-qubit entangling gates are sufficient for universal quantum computing, multiqubit entangling gates can provide significant speedups for quantum algorithms and state preparation. For example, multitarget Rydberg gates [31–35] enable the implementation of Shor’s algorithm in constant time [36]. Conversely, multicontrol Rydberg gates [32,34,37–43] allow for efficient implementations of Grover’s search algorithm [44].

The conventional implementation of the two-qubit Rydberg-blockade gate uses three fundamental steps, with qubit states $|0\rangle, |1\rangle$ encoded in the ground-state manifold [Fig. 1(a)]. (1) A π pulse with Rabi frequency $\Omega_g^{(c)}$ is applied to the first atom (the control atom), which excites the $|0\rangle$ state to a Rydberg state $|c\rangle$. (2) A pulse sequence involving a Rydberg state is applied to the second atom (the

target atom). Here, we consider a 2π pulse with Rabi frequency $\Omega_g^{(t)}$ applied to the $|0\rangle$ state via the Rydberg state $|t\rangle$ (usually, $|t\rangle = |c\rangle$, but this is not necessary). (3) A $-\pi$ pulse with Rabi frequency $\Omega_g^{(c)}$ is applied to the control atom, returning the Rydberg state to the $|0\rangle$ state. When the qubits are in the $|10\rangle$ state, they pick up a minus sign due to

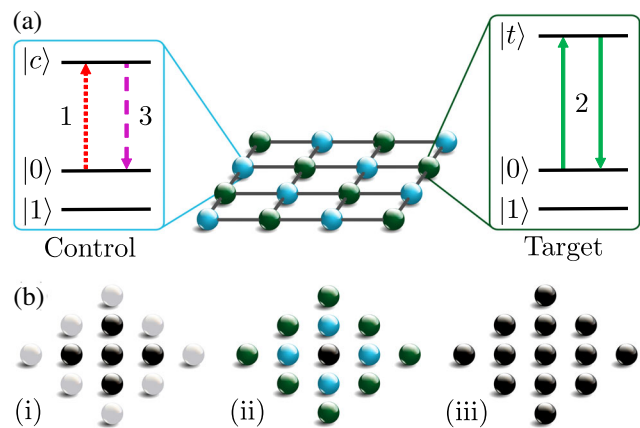


FIG. 1. (a) Pulse sequence to realize controlled-Z gates (see text for details), where light blue (dark green) spheres represent control (target) atoms. The above configuration realizes a C_8Z^8 gate. Other configurations of control and target atoms are possible. (b) Intermediate step of the Greenberger-Horne-Zeilinger (GHZ) state creation. Black (white) spheres indicate atoms that are (not) part of the GHZ state. After the application of a $C_4\text{NOT}^8$ gate in (ii), the GHZ state is increased from (i) 5 to (iii) 13 atoms.

the 2π pulse. Otherwise, the state is left unchanged. By applying a Pauli-X gate to the target qubit before and after the pulse sequence, this realizes the controlled-Z gate (CZ gate), which applies a Pauli-Z gate to the target qubit when the control qubit is in the $|1\rangle$ state.

Many previous approaches to realizing multiqubit Rydberg gates rely on asymmetric Rydberg blockade, in which there is a large separation of scales between different types of Rydberg interactions [5,17,33,38,45,46]. For example, if the control-control interaction is much smaller than the control-target interaction, then control atoms can blockade target atoms without blockading other control atoms, which can be used to engineer a multicontrol gate. In most cases, asymmetric Rydberg blockade was achieved through the use of strong $1/r^3$ dipole-dipole interactions and weaker $1/r^6$ vdW interactions. However, the dipole-dipole interactions are off-diagonal, which can result in many-body resonances and antiblockade, reducing gate fidelity [47]. Moreover, these proposals have been limited to gates involving either many controls or many targets, but not both, which has potential applications for classical verification of quantum computers [48].

In this Letter, we propose a method for engineering gates involving many control qubits and many target qubits. This is accomplished by combining the principles of asymmetric blockade with the conventional two-qubit Rydberg-blockade gate using microwave fields. The use of microwave fields to modify Rydberg interactions has been considered in a variety of contexts [7,11,14,18,46,49–54]. We show that by dressing several Rydberg states with strong microwave fields, perfect asymmetric blockade can be realized, in which intraspecies (control-control and target-target) Rydberg interactions are negligible while interspecies (control-target) Rydberg interactions are large. Moreover, the control-target interactions will be *diagonal* dipole-dipole interactions, preventing many-body resonances from playing a role while still using strong dipole-dipole interactions. We achieve this by applying two microwave drives with different polarizations. Because of a sign difference in the resulting dipole-dipole interaction from each drive, the drives can be tuned so that the intraspecies interactions cancel out with one another. Using the remaining tunability, we can further suppress the intraspecies vdW interactions. Since the intraspecies interactions are negligible, the same pulse sequence can be used as in the two-qubit case. This generalizes the CZ gate to a $C_k Z^m$ gate with k control qubits and m target qubits. If all control qubits are in the $|1\rangle$ state, a Pauli-Z gate is applied to each of the target qubits. Otherwise, the target qubits are unchanged. This can be generalized to realize a $C_k U_1 \cdots U_m$ gate, which applies an arbitrary controlled unitary to each target qubit [55,56]. We conclude with a discussion of the performance of these gates compared to other approaches by considering a $C_8 Z^8$ gate [Fig. 1(a)] and Greenberger-Horne-Zeilinger (GHZ) state preparation. The latter is achieved by sequentially

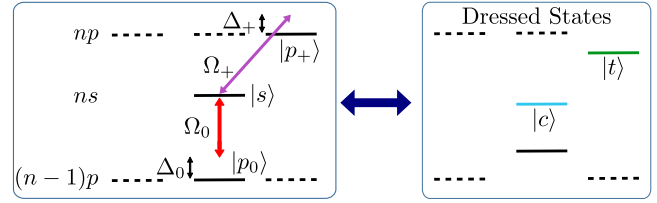


FIG. 2. Dressing scheme for control and target Rydberg states involving one s state ($L = 0$) and two p states ($L = 1$), where n denotes the principal quantum number and dotted lines are not involved in the dressing. The $|s\rangle$ state is coupled to the $|p_0\rangle$ state with Rabi frequency Ω_0 and detuning Δ_0 . The $|s\rangle$ state is coupled to the $|p_+\rangle$ state using Rabi frequency Ω_+ and detuning Δ_+ . The right side of the figure illustrates the resulting dressed states $|c\rangle$, $|t\rangle$, and the third unused dressed state.

applying $C_k \text{NOT}^m$ gates to the k atoms at the edge of the GHZ state and their m nearest neighbors [Fig. 1(b)].

Microwave dressing.—To achieve the desired interactions, we consider the dressing scheme in Fig. 2. This couples a Rydberg s state ($L = 0$) to two Rydberg p states ($L = 1$) with different principal quantum numbers. Although we study a specific dressing scheme, the only requirement is that one microwave field drives a π transition while another microwave field drives a σ transition, which will be used to destructively interfere two interaction terms. Additional drives would provide more tunability. The Hamiltonian for this dressing, in the rotating frame and under the rotating wave approximation, is

$$H_{mw} = -\Delta_0 |p_0\rangle\langle p_0| + \Omega_0 |s\rangle\langle p_0| + \Omega_0^* |p_0\rangle\langle s| - \Delta_+ |p_+\rangle\langle p_+| + \Omega_+ |s\rangle\langle p_+| + \Omega_+^* |p_+\rangle\langle s|, \quad (1)$$

where $\Delta_{0/+} = \nu_{0/+} - \omega_{0/+}$ denotes the detuning of the drives ($\nu_{0/+}$ and $\omega_{0/+}$ are the drive and transition frequencies, respectively) and $\Omega_{0/+}$ the Rabi frequency of the drive from $|s\rangle$ to $|p_{0/+}\rangle$.

Since the s and p states have different orbital angular momenta, the resultant dressed states experience dipole-dipole interactions. In the rotating frame of both microwave fields, atoms i and j interact via

$$V_{dd}^{(i,j)} = \frac{1 - 3 \cos^2 \theta_{ij}}{r_{ij}^3} (\mu_0^2 |s_i p_{j,0}\rangle\langle p_{i,0} s_j| - \mu_+^2 / 2 |s_i p_{j,+}\rangle\langle p_{i,+} s_j|) + \text{H.c.}, \quad (2)$$

where r_{ij} is the distance between atoms i and j , θ_{ij} is the angle the displacement vector makes with the quantization axis, and $\mu_0 = \langle p_0 | d_0 | s \rangle$, $\mu_+ = \langle p_+ | d_+ | s \rangle$ are transition dipole moments, where $d_p = \hat{\mathbf{e}}_p \cdot \mathbf{d}$ is a component of the dipole operator \mathbf{d} and $\hat{\mathbf{e}}_0 = \hat{\mathbf{z}}$, $\hat{\mathbf{e}}_{\pm} = \mp (\hat{\mathbf{x}} \pm i\hat{\mathbf{y}})/\sqrt{2}$. There are additional interaction terms with different angular dependencies that do not preserve total m_L (e.g.,

$|s_i p_{j,+}\rangle\langle p_{i,0} s_j|$) and oscillate with frequencies $2\nu_+$, $2\nu_0$, or $\nu_+ \pm \nu_0$ in the rotating frame. When the two p states are from different p -state manifolds, these interactions can be dropped via the rotating wave approximation, although in other contexts they can be used as a resource to engineer useful interactions [57].

Asymmetric blockade.—Next, we discuss how to design the dressing such that only interspecies interactions are nonzero. Consider a general pair of unnormalized control and target Rydberg states, $|c\rangle$ and $|t\rangle$, which are eigenstates of H_{mw} :

$$|c\rangle \propto |s\rangle + c_0|p_0\rangle + c_+|p_+\rangle, \quad (3a)$$

$$|t\rangle \propto |s\rangle + t_0|p_0\rangle + t_+|p_+\rangle. \quad (3b)$$

For large drive $\Omega_{0/+} \gg V_{dd}$ [58], the two-atom Rydberg states are product states of the one-atom Rydberg states: $|cc\rangle, |tt\rangle, |ct\rangle, |tc\rangle$. This holds for N -atom Rydberg states up to perturbative corrections, which are captured by vdW interactions. The intraspecies interactions for $|c\rangle$ and $|t\rangle$ are

$$V_{cc} = \langle cc|V_{dd}|cc\rangle \propto |c_0|^2\mu_0^2 - |c_+|^2\mu_+^2/2, \quad (4a)$$

$$V_{tt} = \langle tt|V_{dd}|tt\rangle \propto |t_0|^2\mu_0^2 - |t_+|^2\mu_+^2/2, \quad (4b)$$

where the atom indices i, j have been dropped. From this, we see that while it is not possible to nullify the intraspecies interactions using only a single p state, it is possible with two p states. The sign difference is the origin of the requirement that both π - and σ -transition drives are needed. By fixing $|c_+|^2 = 2M^2|c_0|^2$ and $|t_+|^2 = 2M^2|t_0|^2$ where $M = \mu_0/\mu_+$, the intraspecies interactions are 0. Although these two constraints are the same for both states, this does not require $|c\rangle = |t\rangle$ because the phases and magnitudes of the coefficients for the two states can be different.

We must also consider the off-diagonal interactions between $|c\rangle$ and $|t\rangle$. The strength of the only resonant off-diagonal term is related to the two intraspecies interactions $\langle ct|V_{dd}|tc\rangle \propto \mathcal{N}_c^4 V_{cc} + \mathcal{N}_t^4 V_{tt}$, where $\mathcal{N}_{c/t}$ are state normalization factors. As a result, this interaction is zero when the intraspecies interactions are zero. The remaining off-diagonal terms, such as those proportional to $|cc\rangle\langle tt|$, need not be reduced as long as they are sufficiently off-resonant.

Since the interspecies interaction is the source of Rydberg blockade in the gate, it must be large. This interaction is

$$V_{ct} = \langle ct|V_{dd}|ct\rangle \propto c_0 t_0^* \mu_0^2 - c_+ t_+^* \mu_+^2/2 + \text{c.c.} \quad (5)$$

Although this equation is similar to Eq. (4), it differs in that the phases of the coefficients matter. The phases of c_0, c_+ can be absorbed into $|p_0\rangle, |p_+\rangle$, leaving only the phases of

t_0, t_+ free. The intraspecies interaction is maximized when t_0, t_+ are real and have opposite signs.

Additionally, we assume that $|c\rangle$ and $|t\rangle$ come from the same drives, which are applied to all atoms. (The case of different drives is discussed in the Supplemental Material [56].) This enforces the constraint

$$\langle c|t\rangle \propto 1 + t_0 c_0^* + t_+ c_+^* = 0. \quad (6)$$

Taking $c_+ = \sqrt{2}M c_0$ and $t_+ = -\sqrt{2}M t_0$ for real t_0, c_0 , we find

$$t_0 = \frac{1}{(2M^2 - 1)c_0}. \quad (7)$$

As long as $M^2 \neq 1/2$, both dressed states can be realized with the same drives. The values of $\Omega_{0/+}, \Delta_{0/+}$ may be determined, up to an overall scale, by requiring that both states are eigenvectors of H_{mw} . The maximum interspecies interaction under this constraint is

$$V_{ct}^{\max} = \min\left(\frac{\mu_0^2}{\mu_+^2/2}, \frac{\mu_+^2/2}{\mu_0^2}\right)(\mu_0^2 - \mu_+^2/2), \quad (8a)$$

$$c_0^{\max} = |2M^2 - 1|^{-\frac{1}{2}}, \quad (8b)$$

where c_0^{\max} denotes the value of c_0 that realizes this interaction. The min function reflects the fact that the smaller of the two undressed dipole-dipole interactions will set the overall scale of the interaction. Near this maximal interaction strength, the light shifts for $|c\rangle$ and $|t\rangle$ become degenerate, precluding π pulses that excite only one or the other and violating the assumption that several off-diagonal interactions are off-resonant. To avoid these issues, we set $c_0 = \alpha c_0^{\max}$ for $\alpha \neq 1$, removing this degeneracy. While this change reduces the interspecies interaction strength, it remains comparable to the maximal interspecies interaction.

For strong drive, the level structure can lead to additional Rydberg states being dressed, such as when the fine structure is comparable to $\Omega_{0/+}$. Although this modifies H_{mw} and precludes an analytic solution, it nevertheless remains possible to realize asymmetric blockade [56].

Suppressing vdW interactions.—Since we have successfully eliminated the intraspecies dipole-dipole interactions for $|c\rangle$ and $|t\rangle$, intraspecies vdW interactions are relevant. While the dipole-dipole interactions are much larger than the vdW interactions for the same atomic separation, it is important to compare intraspecies interactions at short distances to interspecies interactions at long distances. The target-target vdW interaction is particularly important, as $\Omega_g^{(t)}$ must be simultaneously stronger than the vdW interaction and weaker than the blockade interaction V_{ct} . In contrast, $\Omega_g^{(c)}$ is not limited by V_{ct} . Additionally, it is

important to ensure that the corrections remain perturbative so higher-order processes do not lead to antiblockade and avalanche processes [47,59–62].

The relevant vdW interactions take the form

$$V_{\text{vdW}}^{(i,j)} = -\frac{C_6^{(c)}(\theta_{ij})}{r_{ij}^6} |c_i c_j\rangle \langle c_i c_j| - \frac{C_6^{(t)}(\theta_{ij})}{r_{ij}^6} |t_i t_j\rangle \langle t_i t_j| \\ - \frac{C_6^{(+)}(\theta_{ij})}{r_{ij}^6} |+_ij\rangle \langle +_ij| - \frac{C_6^{(-)}(\theta_{ij})}{r_{ij}^6} |-_ij\rangle \langle -_ij|, \quad (9)$$

where $C_6^{(c)}$, $C_6^{(t)}$, $C_6^{(+)}$, $C_6^{(-)}$ denote the strength of the vdW interactions for $|c\rangle$, $|t\rangle$, and the symmetric or antisymmetric states $|\pm\rangle = (|ct\rangle \pm |tc\rangle)/\sqrt{2}$, respectively, which are a result of second-order nondegenerate perturbation theory [56]. Since the off-resonant coupling strengths and energy differences are dependent on the dressing, the strength of the vdW interactions changes as a function of the dressing, making them tunable [56]. Two degrees of freedom allow this tunability. The first is the overall scale of the dressing fields. By varying H_{mw} by a constant factor, the dressed states remain the same while the light shifts change, modifying the perturbative calculation of C_6 . The second degree of freedom is encoded in α . This picture is not qualitatively modified due to additional coupled states, although the modification to H_{mw} is less trivial.

Most importantly, this allows for the ability to nullify $C_6^{(t)}$. This can be understood by considering the existence of two-atom resonances, which arise when one of the dressed pair states under consideration (e.g., $|cc\rangle$) becomes degenerate with a different Rydberg pair state. At a resonance, the energy difference of the two pair states passes through zero and $C_6^{(t)}$ changes signs, leading to zero crossings due to the presence of multiple resonances. Because of the additional tunable parameter, one may simultaneously identify parameters where the vdW interactions are most perturbative, allowing for stronger interspecies interactions and ensuring the validity of the dressed-state basis (hence $\Omega_{mw} \gg V_{ct}$). In Fig. 3, we illustrate an example that uses this tunability. Because the dipole-dipole interactions have multiple angular dependencies, vdW nullification is only valid for fixed θ_{ij} . This procedure is approximately independent of n aside from overall energy and length scales, and the gate performance is comparable for different n [56].

Gate performance.—There are three primary sources of error: dissipation, vdW interactions, and imperfect blockade. For a square 2π pulse or two square π pulses, the probability of decay for a single Rydberg atom is $\epsilon_\gamma = \pi/2/\Omega_g \tau$, where Ω_g is the Rabi frequency of the pulses and τ is the lifetime of the Rydberg state. The error due to vdW interactions scales as $\epsilon_{\text{vdW}} \sim (V_{\text{vdW}}/\Omega_g)^2$, where V_{vdW} is the total vdW blockade strength. Similarly, the error due to imperfect blockade scales as

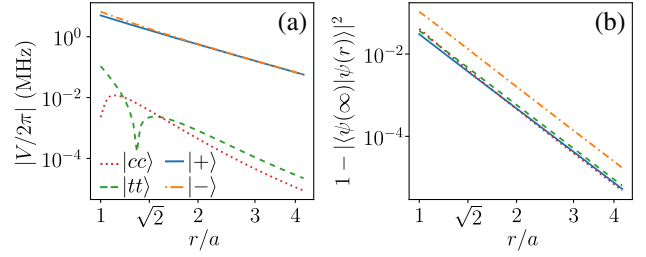


FIG. 3. (a) Dressed interactions and (b) deviations from dressed state basis $1 - |\langle \psi(\infty) | \psi(r) \rangle|^2 \propto r^{-6}$ for $|\psi(\infty)\rangle = |cc\rangle, |tt\rangle, |\pm\rangle$. States dressed are $|s\rangle = |n=60, L=0, J=1/2, m_J=1/2\rangle$, $|p_0\rangle = |n=60, L=1, J=1/2, m_J=1/2\rangle$, $|p_+\rangle = |n=59, L=1, J=1/2, m_J=-1/2\rangle$ of ^{87}Rb for $\theta_{ij} = \pi/2$ using exact diagonalization in a Floquet basis with lattice spacing $a = 5.5 \mu\text{m}$. Dressing parameters are $(\Omega_0, \Delta_0, \Omega_+, \Delta_+)/2\pi = (-265, -223, 176, 200)$ MHz, where a negative Rabi frequency indicates the importance of the relative phase of the drives and determines the light shifts. The effects of coupling to $|p'_0\rangle = |n=60, L=1, J=3/2, m_J=1/2\rangle$, $|p'_+\rangle = |n=59, L=1, J=3/2, m_J=-1/2\rangle$, are also accounted for [56,63]. Interaction fits give $C_3^{(ct)}/2\pi = -730 \text{ MHz } \mu\text{m}^3$ and $(C_6^{(c)}, C_6^{(t)}, C_6^{(+)}, C_6^{(-)})/2\pi = (0.6, -1.8, -17, -64) \text{ GHz } \mu\text{m}^6$ [64] and $|E_c - E_t|/2\pi = 307 \text{ MHz}$. The lifetimes of $|c\rangle$ and $|t\rangle$ are $\tau_c = 431 \mu\text{s}$ and $\tau_t = 356 \mu\text{s}$, respectively [65].

$\epsilon_b \sim (\Omega_g^{(t)}/V_b)^2$, where V_b is the total dipole-dipole blockade strength.

In order to investigate the performance of these gates, we consider two scenarios using the dressing discussed in Fig. 3. In the first, we consider a C_8Z^8 gate on a 4×4 checkerboard lattice [Fig. 1(a)]. We consider the average fidelity [66]

$$\bar{F}(G, U) \equiv \int |\langle \psi | U^\dagger G | \psi \rangle|^2 d\psi, \quad (10)$$

where U is the ideal implementation of the gate, G is the physical implementation of the gate, and the integral is performed over the normalized Haar measure $d\psi$. We have assumed G is unitary since we can treat the dissipation errors separately. Because of the large Hilbert space, we estimate \bar{F} via Haar random sampling of $|\psi\rangle$ [56]. The corresponding error is $1 - \bar{F}$. Optimizing the pulse strengths and phases [56], we find a gate error of 18.5% using $\Omega_g^{(c)}/2\pi = 1 \text{ MHz}$ and $\Omega_g^{(t)}/2\pi = 47 \text{ kHz}$, approximately half of which is due to dissipation. For the C_8Z^8 gate, $\Omega_g^{(t)}$ is comparable to the smallest interspecies interaction. This does not lead to large errors because there are very few input states that have such small blockade strengths, and typically multiple control atoms will provide blockade. If the probability of small V_b is significant, smaller Rabi frequencies should be used. Although this increases the Rydberg dissipation probability, fewer atoms are excited to a Rydberg state, and these

partially balance each other. In general, the larger gates are more suited to implementations where some information is known about the typical V_b . If we consider a 3×3 lattice using $\Omega_g^{(i)} = \min V_b/8$, the C_5Z^4 gate and C_4Z^5 gate have errors of 8.4% and 8.9%, respectively.

In the second scenario, we use these gates to create 13- and 25-atom GHZ states using two or three steps, respectively. This is achieved by using $C_k\text{NOT}^m$ gates, which can be realized by applying single-qubit Hadamard gates to the target qubits before and after the C_kZ^m gate. Initially, all qubits in a square lattice are in $|0\rangle$ except for one, which starts in $(|0\rangle + |1\rangle)/\sqrt{2}$. At each step, the boundary atoms of the GHZ state are used as controls and their outer nearest neighbors as targets [Fig. 1(b)]. The 13- and 25-atom GHZ states have errors of 2.8% and 5.8% [56]. In comparison, Ref. [45] predicts a 16% error for an 8-atom GHZ state via asymmetric blockade. Although two-qubit gates with a theoretical minimal error of 0.3% have comparable errors (3.6% and 7.2%), they require 12 and 24 gates, respectively, as well as much larger Rabi frequencies [2].

Outlook.—We have presented a protocol that uses microwave-dressed Rydberg states to realize gates involving multiple control qubits and multiple target qubits. These gates can be used to simplify quantum protocols, greatly reducing the number of gates needed. While this reduces the need for fault-tolerant error correction, understanding how to realize fault tolerance for complicated multiqubit gates remains an important direction [67,68]. Although we have considered only two drives, these principles can be generalized to many drives, e.g., using locally addressable optical drives to realize local dressing [69], providing superior tunability. Moreover, the application of strong microwave fields provides a new approach to realizing novel, tunable interactions for quantum simulation and could be used for nondestructive cooling by engineering state-insensitive interactions [70] or monitoring quantum simulators with quantum nondemolition couplings [71]. Similarly, it is worth exploring ways to realize multiqubit gates beyond two-qubit generalizations. For example, more general forms of controlled-unitary gates and controlled Hamiltonian evolution, which has potential applications in anyonic interferometry [72], measuring quantum information scrambling [73], quantum phase estimation [74], and quantum metrology with indefinite causal order [75], and which also has close connections to the central spin model [76]. Additionally, these methods have potential applications in speeding up state transfer and the preparation of multiscale entanglement renormalization ansatz using the long-range $1/r^3$ interactions [77,78]. Finally, the ideas presented in this Letter can be applied to other systems with dipole-dipole interactions, such as polar molecules [79–83], magnetic atoms [84–86], and nitrogen-vacancy centers in diamond [87,88].

We thank M. Lukin, G. Alagic, A. Childs, O. Shtanko, L. P. García-Pintos, A. Deshpande, and M. Tran for discussions. J. T. Y., P. B., R. B., and A. V. G. acknowledge support by AFOSR, AFOSR MURI, DoE ASCR Quantum Testbed Pathfinder program (Award No. DE-SC0019040), U.S. Department of Energy Award No. DE-SC0019449, DoE ASCR Accelerated Research in Quantum Computing program (Award No. DE-SC0020312), NSF PFCQC program, ARO MURI, ARL CDQI, and NSF PFC at JQI. J. T. Y. was supported in part by the NIST NRC Research Postdoctoral Associateship Award. A. M. K. acknowledges support by AFOSR and NIST. R. B. acknowledges support by NSERC and FRQNT of Canada.

*Corresponding author.

jeremy.young@colorado.edu

- [1] D. Jaksch, J. I. Cirac, P. Zoller, S. L. Rolston, R. Côté, and M. D. Lukin, *Phys. Rev. Lett.* **85**, 2208 (2000).
- [2] M. Saffman and T. G. Walker, *Phys. Rev. A* **72**, 022347 (2005).
- [3] M. Saffman, T. G. Walker, and K. Mølmer, *Rev. Mod. Phys.* **82**, 2313 (2010).
- [4] T. Xia, X. L. Zhang, and M. Saffman, *Phys. Rev. A* **88**, 062337 (2013).
- [5] E. Brion, A. S. Mouritzen, and K. Mølmer, *Phys. Rev. A* **76**, 022334 (2007).
- [6] M. H. Goerz, E. J. Halperin, J. M. Aytac, C. P. Koch, and K. B. Whaley, *Phys. Rev. A* **90**, 032329 (2014).
- [7] M. M. Müller, D. M. Reich, M. Murphy, H. Yuan, J. Vala, K. B. Whaley, T. Calarco, and C. P. Koch, *Phys. Rev. A* **84**, 042315 (2011).
- [8] M. M. Müller, H. R. Haakh, T. Calarco, C. P. Koch, and C. Henkel, *Quantum Inf. Process.* **10**, 771 (2011).
- [9] M. M. Müller, M. Murphy, S. Montangero, T. Calarco, P. Grangier, and A. Browaeys, *Phys. Rev. A* **89**, 032334 (2014).
- [10] D. Møller, L. B. Madsen, and K. Mølmer, *Phys. Rev. Lett.* **100**, 170504 (2008).
- [11] D. D. B. Rao and K. Mølmer, *Phys. Rev. A* **90**, 062319 (2014).
- [12] I. I. Beterov, M. Saffman, E. A. Yakshina, D. B. Tretyakov, V. M. Entin, G. N. Hamzina, and I. I. Ryabtsev, *J. Phys. B* **49**, 114007 (2016).
- [13] X.-F. Shi, F. Bariani, and T. A. B. Kennedy, *Phys. Rev. A* **90**, 062327 (2014).
- [14] X.-F. Shi and T. A. B. Kennedy, *Phys. Rev. A* **95**, 043429 (2017).
- [15] X.-D. Tian, Y.-M. Liu, C.-L. Cui, and J.-H. Wu, *Phys. Rev. A* **92**, 063411 (2015).
- [16] A. C. J. Wade, M. Mattioli, and K. Mølmer, *Phys. Rev. A* **94**, 053830 (2016).
- [17] H.-Z. Wu, Z.-B. Yang, and S.-B. Zheng, *Phys. Rev. A* **82**, 034307 (2010).
- [18] D. Petrosyan and K. Mølmer, *Phys. Rev. Lett.* **113**, 123003 (2014).
- [19] L. Isenhower, E. Urban, X. L. Zhang, A. T. Gill, T. Henage, T. A. Johnson, T. G. Walker, and M. Saffman, *Phys. Rev. Lett.* **104**, 010503 (2010).

- [20] T. Wilk, A. Gaëtan, C. Evellin, J. Wolters, Y. Miroshnychenko, P. Grangier, and A. Browaeys, *Phys. Rev. Lett.* **104**, 010502 (2010).
- [21] X. L. Zhang, L. Isenhower, A. T. Gill, T. G. Walker, and M. Saffman, *Phys. Rev. A* **82**, 030306(R) (2010).
- [22] K. M. Maller, M. T. Lichtman, T. Xia, Y. Sun, M. J. Piotrowicz, A. W. Carr, L. Isenhower, and M. Saffman, *Phys. Rev. A* **92**, 022336 (2015).
- [23] Y.-Y. Jau, A. M. Hankin, T. Keating, I. H. Deutsch, and G. W. Biedermann, *Nat. Phys.* **12**, 71 (2016).
- [24] Y. Zeng, P. Xu, X. He, Y. Liu, M. Liu, J. Wang, D. J. Papoular, G. V. Shlyapnikov, and M. Zhan, *Phys. Rev. Lett.* **119**, 160502 (2017).
- [25] C. J. Picken, R. Legaie, K. McDonnell, and J. D. Pritchard, *Quantum Sci. Technol.* **4**, 015011 (2018).
- [26] H. Levine, A. Keesling, A. Omran, H. Bernien, S. Schwartz, A. S. Zibrov, M. Endres, M. Greiner, V. Vuletić, and M. D. Lukin, *Phys. Rev. Lett.* **121**, 123603 (2018).
- [27] H. Levine, A. Keesling, G. Semeghini, A. Omran, T. T. Wang, S. Ebadi, H. Bernien, M. Greiner, V. Vuletić, H. Pichler, and M. D. Lukin, *Phys. Rev. Lett.* **123**, 170503 (2019).
- [28] T. M. Graham, M. Kwon, B. Grinkemeyer, Z. Marra, X. Jiang, M. T. Lichtman, Y. Sun, M. Ebert, and M. Saffman, *Phys. Rev. Lett.* **123**, 230501 (2019).
- [29] I. S. Madjarov, J. P. Covey, A. L. Shaw, J. Choi, A. Kale, A. Cooper, H. Pichler, V. Schkolnik, J. R. Williams, and M. Endres, *Nat. Phys.* **16**, 857 (2020).
- [30] C. Zhang, F. Pokorny, W. Li, G. Higgins, A. Pöschl, I. Lesanovsky, and M. Hennrich, *Nature (London)* **580**, 345 (2020).
- [31] M. Müller, I. Lesanovsky, H. Weimer, H. P. Büchler, and P. Zoller, *Phys. Rev. Lett.* **102**, 170502 (2009).
- [32] X.-F. Shi, *Phys. Rev. Applied* **9**, 051001(R) (2018).
- [33] S. L. Su, *Chin. Phys. B* **27**, 110304 (2018).
- [34] M. Khazali and K. Mølmer, *Phys. Rev. X* **10**, 021054 (2020).
- [35] C.-Y. Guo, L.-L. Yan, S. Zhang, S.-L. Su, and W. Li, *Phys. Rev. A* **102**, 042607 (2020).
- [36] P. Hoyer and R. Spalek, *Theory Comput.* **1**, 81 (2005).
- [37] I. I. Beterov, I. N. Ashkarin, E. A. Yakshina, D. B. Tretyakov, V. M. Entin, I. I. Ryabtsev, P. Cheinet, P. Pillet, and M. Saffman, *Phys. Rev. A* **98**, 042704 (2018).
- [38] L. Isenhower, M. Saffman, and K. Mølmer, *Quantum Inf. Process.* **10**, 755 (2011).
- [39] J. Gulliksen, D. B. R. Dasari, and K. Mølmer, *Eur. Phys. J. Quantum Technol.* **2**, 4 (2015).
- [40] S. L. Su, H. Z. Shen, E. Liang, and S. Zhang, *Phys. Rev. A* **98**, 032306 (2018).
- [41] S. E. Rasmussen, K. Groenland, R. Gerritsma, K. Schoutens, and N. T. Zinner, *Phys. Rev. A* **101**, 022308 (2020).
- [42] D. Yu, W. Zhang, J.-m. Liu, S. Su, and J. Qian, *arXiv:2007.11938*.
- [43] Y. He, J.-X. Liu, L.-L. Yan, E. Liang, S.-L. Su, and M. Feng, *arXiv:2010.14704*.
- [44] K. Mølmer, L. Isenhower, and M. Saffman, *J. Phys. B* **44**, 184016 (2011).
- [45] M. Saffman and K. Mølmer, *Phys. Rev. Lett.* **102**, 240502 (2009).
- [46] H. Wu, X.-R. Huang, C.-S. Hu, Z.-B. Yang, and S.-B. Zheng, *Phys. Rev. A* **96**, 022321 (2017).
- [47] T. Pohl and P. R. Berman, *Phys. Rev. Lett.* **102**, 013004 (2009).
- [48] U. Mahadev, in *2018 IEEE 59th Annual Symposium on Foundations of Computer Science (FOCS)* (IEEE, Paris, 2018), Vol. 2018-October, pp. 259–267, <http://dx.doi.org/10.1109/FOCS.2018.00033>.
- [49] P. Bohlouli-Zanjani, J. A. Petrus, and J. D. D. Martin, *Phys. Rev. Lett.* **98**, 203005 (2007).
- [50] D. B. Tretyakov, V. M. Entin, E. A. Yakshina, I. I. Beterov, C. Andreeva, and I. I. Ryabtsev, *Phys. Rev. A* **90**, 041403(R) (2014).
- [51] S. Sevinçli and T. Pohl, *New J. Phys.* **16**, 123036 (2014).
- [52] A. W. Glaetzle, M. Dalmonte, R. Nath, I. Rousochatzakis, R. Moessner, and P. Zoller, *Phys. Rev. X* **4**, 041037 (2014).
- [53] D. W. Booth, J. Isaacs, and M. Saffman, *Phys. Rev. A* **97**, 012515 (2018).
- [54] S. K. Kanungo, J. D. Whalen, Y. Lu, M. Yuan, S. Dasgupta, F. B. Dunning, K. R. A. Hazzard, and T. C. Killian, *arXiv:2101.02871*.
- [55] A. Barenco, C. H. Bennett, R. Cleve, D. P. DiVincenzo, N. Margolus, P. Shor, T. Sleator, J. A. Smolin, and H. Woerner, *Phys. Rev. A* **52**, 3457 (1995).
- [56] See Supplemental Material at <http://link.aps.org/supplemental/10.1103/PhysRevLett.127.120501> for details on generalizing to controlled-unitary gates, a discussion of the case of different drives for control and target atoms, analytic expressions for the dressing parameters, a discussion of the effect of coupling to additional states, a detailed derivation of the perturbative vdW interactions, a discussion of sources of error in the gates, and details for the GHZ state preparation protocol.
- [57] A. W. Glaetzle, M. Dalmonte, R. Nath, C. Gross, I. Bloch, and P. Zoller, *Phys. Rev. Lett.* **114**, 173002 (2015).
- [58] Sufficiently large microwave Rabi frequencies are achievable since the expectation value of the dipole operator scales like n^2 .
- [59] E. A. Goldschmidt, T. Boulier, R. C. Brown, S. B. Koller, J. T. Young, A. V. Gorshkov, S. L. Rolston, and J. V. Porto, *Phys. Rev. Lett.* **116**, 113001 (2016).
- [60] J. A. Aman, B. J. DeSalvo, F. B. Dunning, T. C. Killian, S. Yoshida, and J. Burgdörfer, *Phys. Rev. A* **93**, 043425 (2016).
- [61] T. Boulier, E. Magnan, C. Bracamontes, J. Maslek, E. A. Goldschmidt, J. T. Young, A. V. Gorshkov, S. L. Rolston, and J. V. Porto, *Phys. Rev. A* **96**, 053409 (2017).
- [62] J. T. Young, T. Boulier, E. Magnan, E. A. Goldschmidt, R. M. Wilson, S. L. Rolston, J. V. Porto, and A. V. Gorshkov, *Phys. Rev. A* **97**, 023424 (2018).
- [63] S. Weber, C. Tresp, H. Menke, A. Urvoy, O. Firstenberg, H. P. Büchler, and S. Hofferberth, *J. Phys. B* **50**, 133001 (2017).
- [64] Deviations from vdW interactions are due to C_9 , C_{12} interactions.
- [65] N. Šibalić, J. Pritchard, C. Adams, and K. Weatherill, *Comput. Phys. Commun.* **220**, 319 (2017).
- [66] M. A. Nielsen, *Phys. Lett. A* **303**, 249 (2002).
- [67] J. Preskill, *Proc. R. Soc. Ser. A Math. Phys. Eng. Sci.* **454**, 385 (1998).

- [68] D. Aharonov and M. Ben-Or, *SIAM J. Comput.* **38**, 1207 (2008).
- [69] S. de Léséleuc, D. Barredo, V. Lienhard, A. Browaeys, and T. Lahaye, *Phys. Rev. Lett.* **119**, 053202 (2017).
- [70] R. Belyansky, J. T. Young, P. Bienias, Z. Eldredge, A. M. Kaufman, P. Zoller, and A. V. Gorshkov, *Phys. Rev. Lett.* **123**, 213603 (2019).
- [71] D. V. Vasilyev, A. Grankin, M. A. Baranov, L. M. Sieberer, and P. Zoller, *Phys. Rev. X Quantum* **1**, 020302 (2020).
- [72] L. Jiang, G. K. Brennen, A. V. Gorshkov, K. Hammerer, M. Hafezi, E. Demler, M. D. Lukin, and P. Zoller, *Nat. Phys.* **4**, 482 (2008).
- [73] B. Swingle, G. Bentsen, M. Schleier-Smith, and P. Hayden, *Phys. Rev. A* **94**, 040302(R) (2016).
- [74] T. E. O'Brien, B. Tarasinski, and B. M. Terhal, *New J. Phys.* **21**, 023022 (2019).
- [75] X. Zhao, Y. Yang, and G. Chiribella, *Phys. Rev. Lett.* **124**, 190503 (2020).
- [76] W. Yao, R.-B. Liu, and L. J. Sham, *Phys. Rev. B* **74**, 195301 (2006).
- [77] Z. Eldredge, Z.-X. Gong, J. T. Young, A. H. Moosavian, M. Foss-Feig, and A. V. Gorshkov, *Phys. Rev. Lett.* **119**, 170503 (2017).
- [78] M. C. Tran, C.-F. Chen, A. Ehrenberg, A. Y. Guo, A. Deshpande, Y. Hong, Z.-X. Gong, A. V. Gorshkov, and A. Lucas, *Phys. Rev. X* **10**, 031009 (2020).
- [79] S. F. Yelin, K. Kirby, and R. Côté, *Phys. Rev. A* **74**, 050301(R) (2006).
- [80] K.-K. Ni, T. Rosenband, and D. D. Grimes, *Chem. Sci.* **9**, 6830 (2018).
- [81] E. R. Hudson and W. C. Campbell, *Phys. Rev. A* **98**, 040302(R) (2018).
- [82] H. P. Büchler, A. Micheli, and P. Zoller, *Nat. Phys.* **3**, 726 (2007).
- [83] A. V. Gorshkov, S. R. Manmana, G. Chen, E. Demler, M. D. Lukin, and A. M. Rey, *Phys. Rev. A* **84**, 033619 (2011).
- [84] A. Griesmaier, J. Werner, S. Hensler, J. Stuhler, and T. Pfau, *Phys. Rev. Lett.* **94**, 160401 (2005).
- [85] M. Lu, N. Q. Burdick, S. H. Youn, and B. L. Lev, *Phys. Rev. Lett.* **107**, 190401 (2011).
- [86] K. Aikawa, A. Frisch, M. Mark, S. Baier, A. Rietzler, R. Grimm, and F. Ferlaino, *Phys. Rev. Lett.* **108**, 210401 (2012).
- [87] A. Bermudez, F. Jelezko, M. B. Plenio, and A. Retzker, *Phys. Rev. Lett.* **107**, 150503 (2011).
- [88] F. Dolde, I. Jakobi, B. Naydenov, N. Zhao, S. Pezzagna, C. Trautmann, J. Meijer, P. Neumann, F. Jelezko, and J. Wrachtrup, *Nat. Phys.* **9**, 139 (2013).